

Theory of phase conjugation of light in disordered nonlinear media

V. E. Kravtsov, V. I. Yudson, and V. M. Agranovich

*Institute of Spectroscopy, Academy of Sciences of the U.S.S.R., Troitsk, 142 092 Moscow District,
Union of Soviet Socialist Republics*

(Received 10 July 1989)

In the case of disordered nonlinear media, it is shown that in four-wave mixing a phenomena analogous to phase conjugation may occur. In contrast to the case of transparent media in which two counterpropagating pump waves (with frequency ω_p) are required, phase conjugation may occur in the presence of a single pump wave injected into the disordered nonlinear material. We find that in the angular distribution of radiation of frequency ω_s ($\omega_s = 2\omega_p - \omega_i$, where ω_i is the frequency of probe wave) there is a narrow peak in the backscattered direction associated with the probe wave. The intensity of this peak may be some orders of magnitude larger than the diffuse background at the frequency ω_s .

I. INTRODUCTION

Recently, the optics of disordered media has attracted considerable attention. A problem of particular interest has been the study of coherent-wave phenomena originating in multiple scattering. The importance of such effects was realized in the theory of Anderson localization of electrons in disordered conductors.¹ Well-known examples of such effects in linear optics are backscattering enhancement of light scattered by a disordered medium,^{2,3} as well as reproducible random variations of light intensity with scattering angle (referred to as a "speckle pattern"⁴). Lately the importance of coherent phenomena in nonlinear optics of disordered media has been discussed for the case of three-wave mixing.⁵ There it was shown that interference originating in multiple scattering results in the appearance of new peaks in the angular distribution of light produced by three-wave mixing. However, these peaks were shown to be created by photons generated in the surface region, in a layer with depth of the order of the elastic mean free path l . On the contrary, the diffuse background in the angular distribution is proportional to the whole volume of the sample. Therefore, in samples with thickness $L \gg l$, the peaks are relatively small and could be observed only in the time domain, at a short time delay.⁵

A completely different situation will be shown here to take place in four-wave mixing in disordered media. In addition to weak peculiarities in an angular distribution of generated light which are due to the mixing process in the surface region (similar to that for three-wave mixing⁵), new intense peaks are predicted to occur which originate in the mixing processes in the bulk. We will show that this occurs for the process analogous to the phase-conjugation (PC) process; that is, the generation of light with frequency $\omega_s = 2\omega_p - \omega_i$, where ω_p and ω_i are the frequencies of pump and probe waves, respectively.

The problem of PC in disordered media was discussed recently by Hanamura.⁶ However, in this work PC is supposed to occur in a model of free-boson excitations linearly coupled with external light and scattered by stat-

ic imperfections. Thus it is not clear where the optical nonlinearity essential to the production of the PC wave enters the analysis of Hanamura.⁶ In our opinion, what is explored in Ref. 6 is disorder-induced correlations in the linear scattering of several waves. Note also that the pump waves [$\omega_p = \frac{1}{2}(\omega_i + \omega_s)$] are supposed to be unscattered in Ref. 6, which does not seem natural in the case considered when both waves ω_s and ω_i undergo strong scattering.

Below we consider the most natural case, where the mean free paths of all the waves involved (with close frequencies $\omega_i \approx \omega_p \approx \omega_s$) are equal. In the case of the disordered medium explored here, it is not necessary to consider the standard PC geometry with two counterpropagating pump waves. The reason is that the geometry's "memory" of the direction of the incident wave vector decays through the distance of the order of $l \ll L$ from the surface. Therefore, the simplest and most natural geometry of a PC experiment in disordered media is that with a *single* pump wave. In contrast to the case of transparent media, the presence of a single incident pump wave is sufficient for the PC process because in the bulk of the sample the scattered pump field contains components with all directions of the wave vector. A similar geometry was used in the experiment⁷ for the simple limiting case of weak scattering $l \gg L$. Here we develop the theory for a much more interesting and complicated case of multiple scattering, $l \ll L$.

For this case, we find that in the angular distribution of radiation at frequency ω_s the nonlinear interaction produces a narrow peak in the backscattering direction associated with the probe wave of frequency ω_i . The intensity of this peak may be some orders of magnitude larger than the diffuse background at the frequency ω_s , in contrast to the well-known case of linear backscattering where only at most a factor of 2 is realized. For the case of the nondegenerate PC process ($\omega_i \neq \omega_p$) one can, in principle, distinguish the relatively small nonlinear backscattering peak (ω_s) from the presence of the intense diffuse backgrounds produced by linear scattering of the pump (ω_p) and probe (ω_i) waves.

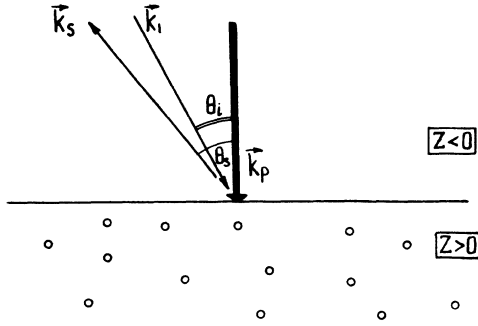


FIG. 1. Experimental geometry.

II. FORMULATION OF THE PROBLEM

The experimental geometry is shown in Fig. 1. A disordered nonlinear medium occupies the half-space $z > 0$. The probe wave of frequency ω_i and the intense pump wave of frequency ω_p are incident from the outside with incident angles θ_i and θ_p , respectively (below, for simplicity, we suppose $\theta_p = 0$).

The quantity of interest is the angular dependence of the differential cross section of nonlinear scattering $d\sigma(\theta_s)/d\Omega$ (θ_s denotes scattering angle) averaged over realizations of disorder:

$$\frac{d\sigma(\theta_s)}{d\Omega} = \frac{\langle \mathbf{S}(\omega_s) \cdot \mathbf{n} \rangle}{S(\omega_i)}, \quad (1)$$

where $\mathbf{S}(\omega_s) \cdot \mathbf{n}$ is an energy flux at the frequency ω_s in the direction \mathbf{n} , and $S(\omega_i)$ is the energy flux of the probe wave. Below we neglect the vectorial nature of the electromagnetic field and consider scalar monochromatic fields with complex amplitudes $E_\alpha(\mathbf{r})$ ($\alpha = i, s, p$).

Such a simplification is valid to an accuracy of some numerical prefactors for the case under consideration, namely the case of coincident polarizations of probe and signal waves. The generation of the signal wave is described by the following equation:

$$\left[\nabla^2 + \frac{\omega_s^2}{c^2} \epsilon_s(\mathbf{r}) \right] E_s(\mathbf{r}) = \eta \frac{\omega_s^2}{c^2} E_p^2(\mathbf{r}) E_i^*(\mathbf{r}), \quad (2)$$

η being the nonlinear susceptibility and the fields E_p, E_i being created by external sources I_p, I_i :

$$\left[\nabla^2 + \frac{\omega_\alpha^2}{c^2} \epsilon_\alpha(\mathbf{r}) \right] E_\alpha(\mathbf{r}) = I_\alpha(\mathbf{r}) \quad \text{with } \alpha = p, i. \quad (3)$$

The source functions vanish within the disordered medium, of course. The disorder is described by a small random part $\delta\epsilon(\mathbf{r})$ of the dielectric function $\epsilon_\alpha(\mathbf{r})$:

$$\epsilon_\alpha(\mathbf{r}) = \epsilon_\alpha + \delta\epsilon(\mathbf{r}). \quad (4)$$

Below we suppose $\delta\epsilon(\mathbf{r})$ to be a Gaussian δ -correlated random field, with a zero average and a correlation function given by

$$\frac{\omega^4}{c^4} \langle \delta\epsilon(\mathbf{r}) \delta\epsilon(\mathbf{r}') \rangle = \frac{4\pi}{l} \delta(\mathbf{r} - \mathbf{r}'). \quad (5)$$

The parameter l will be shown to be equal to the elastic mean free path.

III. THE ANGULAR DISTRIBUTION OF THE SIGNAL-WAVE INTENSITY

The signal field E_s is expressed in terms of the retarded \mathcal{G} and advanced \mathcal{G}^* Green functions of Eqs. (2) and (3) and may be written in the following symbolic form:

$$E_s = \eta \frac{\omega_s^2}{c^2} \mathcal{G}_s [(\mathcal{G}_p I_p)^2 (\mathcal{G}_i^* I_i^*)]. \quad (6)$$

Here the Green functions $\mathcal{G}_\alpha(\mathbf{r}, \mathbf{r}')$ depend on a particular realization of the random field $\delta\epsilon(\mathbf{r})$. They are represented by dark solid lines in Fig. 2(a), which illustrates expression (6); a circle corresponds to the nonlinear vertex, and the points at the ends of the lines correspond to the sources I_α . According to Eq. (1), one should average the quantity $S \sim E_s^* E_s$ over disorder. This quantity is quadratic in the signal field and therefore involves eight Green functions $\mathcal{G}, \mathcal{G}^*$. This averaging is carried out in a conventional way^{3,8} and may be represented by typical diagrams [Figs. 2(b)–2(e)]. Solid lines in the diagrams correspond to averaged Green functions. In the bulk region they are given by an expression:

$$G_\alpha(\mathbf{r}, \mathbf{r}') \equiv \langle \mathcal{G}_\alpha(\mathbf{r}, \mathbf{r}') \rangle = \frac{\exp[(ik_\alpha - 1/2l)|\mathbf{r} - \mathbf{r}'|]}{4\pi|\mathbf{r} - \mathbf{r}'|}, \quad (7)$$

where $k_\alpha = (\omega_\alpha/c) \sqrt{\epsilon_\alpha}$ ($\alpha = i, p, s$). Dashed lines in Fig. 2 correspond to the correlation function (5). Each of the sets consisting of the three dashed lines represents the

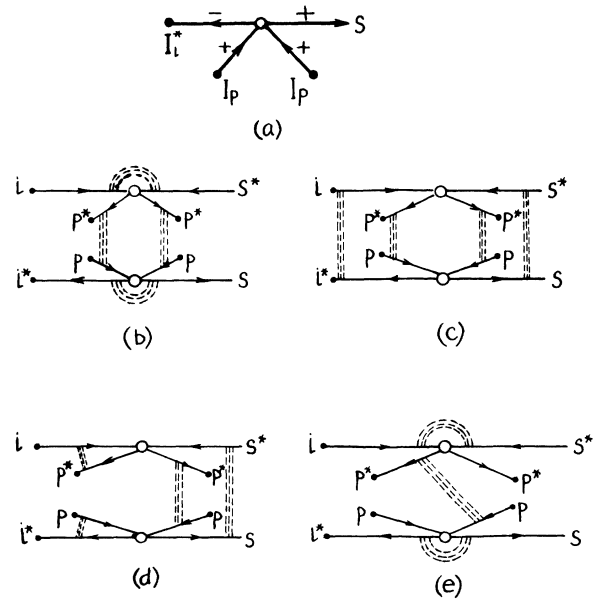


FIG. 2. Diagrams contributing to the intensity of generated light: (a) unaveraged amplitude of the signal wave, symbols + and - label \mathcal{G} and \mathcal{G}^* , respectively; (b) averaged intensity of backscattered peak; (c) averaged diffuse background intensity; (d) interference of pump and probe waves; (e) an example of a surface contribution to the backscattered peak intensity.

infinite series of ladder or maximally crossed diagrams (referred to as diffusion propagators and Cooper particle-particle diffusion propagators), which describe the diffuse propagation of light in a disordered medium. Figures 2(b)–2(e) describe the PC process of interest, to the lowest order in the parameter λ/l (λ is a wavelength). The external lines connected with the sources give the averaged value of incident electric fields within the sample:

$$(G_\alpha I_\alpha)_r = \langle E_\alpha(\mathbf{r}) \rangle = t_\alpha E_\alpha^{(0)} e^{i\mathbf{k}_\alpha \cdot \mathbf{r} - z/2l}, \quad (8)$$

where t_α is a transmission amplitude for the light wave incident on the sample from the outside. In calculating the flux of the signal light radiated from a unit area, it is convenient to prescribe the factor

$$F_s = \frac{t_s}{4\pi\sqrt{A}} \exp\left[i\mathbf{k}_s \cdot \mathbf{r} - \frac{z}{2l}\right], \quad (9)$$

to external lines corresponding to the signal waves. In Eq. (9) A is the surface area and \mathbf{k}_s is a wave vector of the signal field within the media, \mathbf{k}_s being related via the refraction law to the wave vector $n\omega_s/c$ in the direction of the outgoing signal wave.

The diffusion propagators and Cooper particle-particle diffusion propagators are given by

$$C(\mathbf{r}, \mathbf{r}') = \frac{12\pi D}{l^3} \mathcal{D}(\mathbf{r}, \mathbf{r}'), \quad (10)$$

where the diffusion propagator $\mathcal{D}(\mathbf{r}, \mathbf{r}')$ obeys the equation

$$(i\Delta\omega + D\nabla^2)\mathcal{D}(\mathbf{r}, \mathbf{r}') = -\delta(\mathbf{r} - \mathbf{r}') \quad (11)$$

and an effective boundary condition^{5,9} at $z=0$:

$$\mathcal{D}(\mathbf{r}, \mathbf{r}') - hl \frac{\partial}{\partial z} \mathcal{D}(\mathbf{r}, \mathbf{r}') = 0. \quad (12)$$

In Eqs. (10)–(12), D is the diffusion coefficient for photons in a disordered medium, h is a dimensionless phenomenological constant⁹ dependent on the reflectivity of the surface, and $\Delta\omega = \omega_\alpha - \omega_{\alpha'}$ is the difference between frequencies corresponding to Green functions \mathcal{G} and \mathcal{G}^* in a ladder series.

The calculation of Fig. 2(b) is straightforward and results in the following expression for the differential cross section:

$$\frac{d\sigma}{d\Omega} = \frac{B}{|1 + hQ| \operatorname{Re} Q}. \quad (13)$$

Here

$$Q = l(q^2 \cos^2 \theta_i - iL\Delta\omega^{-2})^{1/2}, \quad q = 2\frac{\omega}{c} \sin\left[\frac{\theta_i - \theta_s}{2}\right], \quad (14)$$

where

$$L_{\Delta\omega} = l(|\omega_i - \omega_s| \tau)^{-1/2} \quad (15)$$

is assumed to obey the inequality $L_{\Delta\omega} \gg l$, τ being the time of the mean free path. The factor B in Eq. (13) is given by

$$B = \frac{81}{8\pi} [T_p(h+1)]^2 T_i T_s (\delta n_{\text{NL}})^2 \left[\frac{\omega_s}{c} l\right]^2 (h + \cos\theta_i)^2, \quad (16)$$

where $T_\alpha = |t_\alpha|^2$, and $\delta n_{\text{NL}} = \eta |E_p^{(0)}|^2 n_p^{-1}$ is a nonlinear correction to the pump-wave refractive index n_p .

It is seen from Eqs. (13)–(16) that the dimensionless cross section $d\sigma(\theta_s)/d\Omega$ exhibits a sharp peak at the scattering angle $\theta_s \approx \theta_i$ (backscattering), the peak width being

$$\Delta\theta = \frac{\lambda}{2\pi L_{\Delta\omega} \cos\theta_i} \ll \frac{\lambda}{2\pi l}. \quad (17)$$

At $(\omega_i - \omega_s)\tau \rightarrow 0$, the width decreases, the peak intensity increases, and the integral peak intensity σ_{peak} remains constant. The intensity integrated over the solid angle has the form

$$\sigma_{\text{peak}} \sim (\delta n_{\text{NL}})^2 \frac{2\pi l}{\lambda}. \quad (18)$$

Results (13)–(18) are valid for a semi-infinite sample in the absence of absorption. At a finite sample thickness L ($L \gg l$) or at a finite mean free path l_{in} ($l_{\text{in}} \gg l$) limited by absorption, one should replace $L_{\Delta\omega}$ in Eqs. (15) and (17) by $\min\{L_{\Delta\omega}, L, \sqrt{l_{\text{in}}}\}$. In particular, at $\omega_i - \omega_s \rightarrow 0$ and $l_{\text{in}} \rightarrow \infty$ the peak intensity is proportional to the sample thickness L . This allows one to consider this nonlinear backscattering process as a bulk effect.

Figure 2(c) describes a bulk contribution to the diffuse background intensity at frequency ω_s . Using Eqs. (8) and (9) one can readily verify that this contribution is isotropic and does not depend on the direction of incidence of the probe wave. In addition, this contribution is not sensitive to a small difference of frequencies $\omega_i - \omega_p$ because of the equality $\Delta\omega = 0$ for all the ladders of Fig. 2(c). Therefore, the diffuse background intensity is proportional to an effective thickness of the sample:

$$L_0 = \min\{L, \sqrt{l_{\text{in}}}\}. \quad (19)$$

For the ratio of the backscattering peak intensity $I_{\text{peak}}(\omega_s)$ at $\theta_s = \theta_i$ and that of the diffuse background $I_0(\omega_s)$, we have obtained the following estimate:

$$\frac{I_{\text{peak}}(\omega_s)}{I_0(\omega_s)} \sim \frac{2\pi l}{\lambda} \frac{L_{\Delta\omega}}{L_0}. \quad (20)$$

At sufficiently small values of $\Delta\omega$ and λ/l this ratio may be large. It should be stressed that this peak could be observed only with a high-angular-resolution technique. The reason is that the integrated background intensity σ_0 considerably exceeds that for the backscattering peak:

$$\sigma_0 \sim \frac{L_0}{l} \sigma_{\text{peak}}. \quad (21)$$

The contributions of Figs. 2(b) and 2(c) considered above do not depend on the relative directions of the wave vectors \mathbf{k}_p and \mathbf{k}_i (see Fig. 1). On the contrary, Fig. 2(d) exhibits such a dependence. However, at $|\mathbf{k}_p - \mathbf{k}_i| \gg l^{-1}$ (i.e., at not overly small values of θ_i) all diagrams of 2(d) type turn out to be small by the amount of the parameter λ/l .

Up to now we discussed the diagrams with four diffusion propagators and/or Cooper particle-particle diffusion propagators. Extra diffusion propagators (Cooper particle-particle diffusion propagators) result in the additional small factor λ/l . On the other hand, using a small number of diffusion propagator and Cooper particle-particle diffusion propagators [see, e.g., Fig. 2(e)] one deals with diagrams describing the surface contribution and, hence, those that are small by the amounts of parameters l/L_0 or $l/L_{\Delta\omega}$. Indeed, in contrast to Figs. 2(b) and 2(d), in Fig. 2(e) the region of nonlinear mixing is not separated from the surface sources by the infinite sequence of scattering events and therefore this region is confined to the surface layer of width l .

IV. DISCUSSION

According to Eqs. (14)–(17) the shape of the PC backscattering peak in a disordered medium differs strongly from that for linear backscattering. If the specular reflectivity of the surface is not too large and the parameter h in Eqs. (12) and (13) is of the order of unity, then the shape of the PC peak at $|\theta_i - \theta_s| \ll 1$ is expressed by

$$\frac{d\sigma(\theta_s)}{d\Omega} \sim ((\theta_i - \theta_s)^2 + [(\theta_i - \theta_s)^4 + (\Delta\theta)^4]^{1/2})^{-1/2}, \quad (22)$$

where the peak width $\Delta\theta$ given by Eq. (17) turns out to be considerably smaller than that for linear backscattering.

Another characteristic feature of nonlinear backscattering is the relative smallness of the diffuse background intensity $I_0(\omega_s)$ as compared to the PC peak intensity $I_{\text{peak}}(\omega_s)$ [see Eq. (20)] at a proper choice of system parameters. Thus, in contrast to linear backscattering (where $I_{\text{peak}}/I_0 = 2$), there is no universal relationship between peak and background intensities for the nonlinear backscattering considered here.

The qualitative explanation of this fact may be given in terms of photon trajectories, i.e., sequences of scattering events. In case of linear backscattering, any pair of photon trajectories connected with time-reversal transformation contributes both to the peak and background intensities. For nonlinear mixing the backscattering peak and the diffuse background are determined by completely different trajectories [see Fig. 3(a) for backscattering and Fig. 3(b) for diffuse background].

Another fact which should be explained is that a set of special trajectories [Fig. 3(a)] (containing, say, N trajectories) may give a larger contribution than a much richer set of general trajectories [Fig. 3(b)] (containing N^2 trajectories). The reason is that due to the phase conjugation for a trajectory [Fig. 3(a)], the phase of the outgoing signal wave does not depend on a particular choice of this trajectory (for given trajectories of pump photons). Therefore, the amplitudes of outgoing signal waves corresponding to these N trajectories are added coherently to give the contribution into the intensity proportional to N^2 . On the other hand, for Fig. 3(b) the phase of the outgoing signal wave depends on a particular trajectory.

The contributions to the intensity of the outgoing wave given by different trajectories [Fig. 3(b)] are incoherent. Thus, the total contribution of N^2 trajectories [Fig. 3(b)]

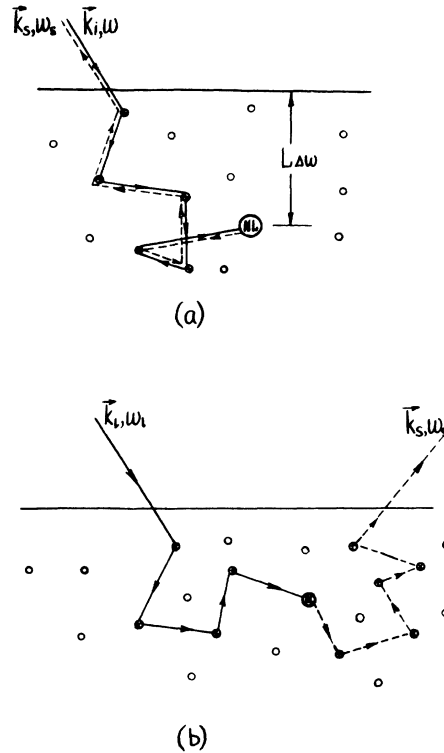


FIG. 3. Trajectories of the probe and signal photons contributing to (a) the backscattered peak and (b) the diffuse background.

is proportional to N^2 and the ratio of the contributions depicted in Figs. 3(a) and 3(b) remains finite in the macroscopic limit $N \rightarrow \infty$.

To explain qualitatively the value of this ratio, one should consider in detail the process of wave mixing in a relatively small region of size $\sim l$. This process is illustrated by Figs. 4(a) and 4(b), which correspond to the tra-

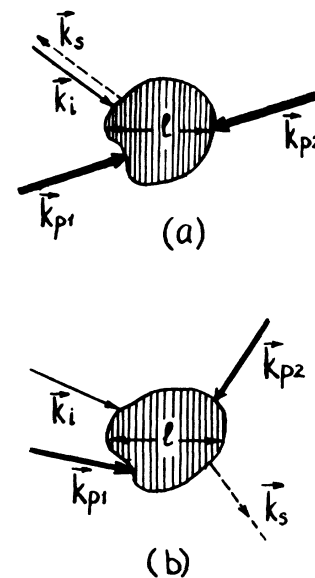
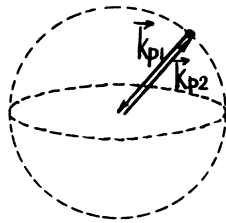


FIG. 4. Processes of four-wave mixing contributing to (a) the backscattered peak and (b) the diffuse background.

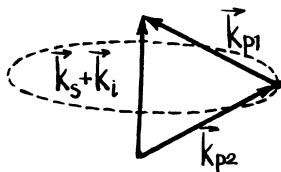
jectories in Figs. 3(a) and 3(b), respectively. The wave vectors involved in the process should obey the phase-matching condition valid to the accuracy of the wave-vector uncertainty in the region of a size $l \gg \lambda$:

$$|\mathbf{k}_i + \mathbf{k}_s + \mathbf{k}_{p1} + \mathbf{k}_{p2}| \lesssim 1/l. \quad (23)$$

As the pump waves 1 and 2 in Figs. 4(a) and 4(b) are completely incoherent in a disordered medium, the contribution of the process depicted in Figs. 4(a) and 4(b) to the outgoing-signal-wave intensity is just proportional to the volume in momentum space constrained by the inequality (23) at fixed values of the wave vectors of the probe \mathbf{k}_i and signal \mathbf{k}_s waves, and the absolute values of the wave vectors \mathbf{k}_{p1} and \mathbf{k}_{p2} . For the backscattering peak generation [Fig. 4(a)] we have $\mathbf{k}_i + \mathbf{k}_s \approx 0$; in this case the volume considered is proportional to the area $\sim \lambda^{-2}$ of a sphere of the radius $|\mathbf{k}_p| \sim \lambda^{-1}$ [see Fig. 5(a)]. For the background generation [Fig. 4(b)] when $|\mathbf{k}_i + \mathbf{k}_s| \sim \lambda^{-1}$, the volume is proportional to the circumference $\sim \lambda^{-1}$ [see Fig. 5(b)]. The correct dimension in both cases is provided by the factor l to the proper powers. Therefore, the ratio of the peak and background intensities may be estimated as $I_{\text{peak}}(\omega_s)/I_0(\omega_s) \sim l/\lambda$, which is in agreement with Eq. (20) up to the factor $L_{\Delta\omega}/L$. The latter factor reflects the fact that the constructive interference of the trajectories [Fig. 3(a)] takes place only if the difference between the phases acquired by the propagating probe and signal waves due to the difference between frequencies ω_i and ω_s is not too large. This requirement restricts the total length of a trajectory [Fig. 3(a)] by the value $\mathcal{L}_{\Delta\omega} = c/|\omega_i - \omega_s|$. Introducing the mean diameter $L_{\Delta\omega} \sim (\mathcal{L}_{\Delta\omega}l)^{1/2}$ of a random-walk trajectory (with a step l) of length $\mathcal{L}_{\Delta\omega}$, one obtains for $L_{\Delta\omega}$ an estimation which



(a)



(b)

FIG. 5. Regions in the momentum space corresponding to processes shown in Figs. 4(a) and 4(b), respectively.

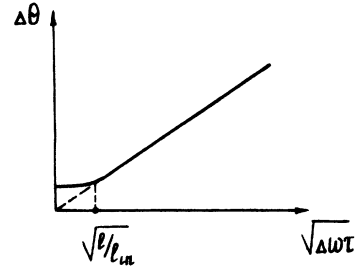


FIG. 6. The angular width $\Delta\theta$ of the backscattered peak vs $\sqrt{\Delta\omega} \equiv \sqrt{|\omega_i - \omega_p|}$.

coincides with Eq. (15). Thus, the backscattering peak intensity is contributed by trajectories [Fig. 3(a)] confined in a layer of the thickness $L_{\Delta\omega}$, while the diffuse background is contributed by the whole sample.

The characteristic feature of the nonlinear process considered is that the parameters of the backscattering peak are sensitive to a small difference $\Delta\omega = \omega_i - \omega_p$. In particular, the angular width of the peak (17) as a function of $\sqrt{|\Delta\omega|}$ is plotted in Fig. 6. The crossover from linear to constant behavior is expected at

$$\sqrt{|\Delta\omega|}\tau \sim l/L_0, \quad (24)$$

where $L_0 = \min\{L, \sqrt{ll_{\text{in}}}\}$. For a semi-infinite sample, relation (24) is reduced to $\Delta\omega \sim c/l_{\text{in}}$. The slope of the linear behavior in the $\sqrt{\Delta\omega}$ part of Fig. 6 equals $\sim \lambda/\sqrt{cl}$. Thus, the dependence of the peak width on the difference between frequencies allows one to find both l and l_{in} . It is also worth noting that when approaching the Anderson localization point, the length L_0 in Eq. (24) should be replaced by the localization radius L_{loc} , provided that $L_{\text{loc}} < L_0$. If the experimental value of L_0 determined by Eq. (24) turns out to be much smaller than the value of $\min\{L, \sqrt{ll_{\text{in}}}\}$ obtained independently, such an experiment may be considered to be evidence in favor of the Anderson localization of photons.

V. CONCLUSION

In conclusion, we summarize the main results of the article.

(1) The disorder induces the phase-conjugation process in the presence of a probe wave and a single pump wave.

(2) There exists a sharp backscattering peak at the signal frequency ω_s in the direction opposite that for the probe wave.

(3) There is no universal relation between the intensities of the backscattering peak $I_{\text{peak}}(\omega_s)$ and the diffuse background $I_0(\omega_s)$ at the frequency ω_s . In particular, the ratio $I_{\text{peak}}(\omega_s)/I_0(\omega_s)$ may be large.

(4) In contrast to linear backscattering, the shape of the nonlinear backscattering peak is mainly determined by the scattering process in the bulk of a sample rather than in the surface layer of thickness l .

(5) The width of the backscattering peak is sensitive to a small difference in the frequencies, $\omega_i - \omega_p$, of incident waves. Such dependence can be a test for the Anderson localization of photons.

ACKNOWLEDGMENTS

We are grateful to Professor D. L. Mills for useful discussions.

¹P. A. Lee and T. V. Ramakrishnan, *Rev. Mod. Phys.* **57**, 287 (1985).

²V. I. Tatarski, *The Effect of a Turbulent Atmosphere on Wave Propagation* (National Technical Information Service, Washington, D.C., 1971).

³E. Akkermans, P. E. Wolf, R. Maynard, and G. Maret, *J. Phys. (Paris)* **49**, 77 (1988).

⁴H. Kaveh, M. Rosenbluh, I. Edrei, and I. Freund, *Phys. Rev. Lett.* **57**, 2049 (1986).

⁵V. M. Agranovich and V. E. Kravtsov, *Phys. Lett. A* **131**, 378

386 (1988).

⁶E. Hanamura, *Phys. Rev. B* **39**, 1152 (1989).

⁷N. F. Pilipetskii, V. I. Popovichev, and V. V. Ragulskii, *Dokl. Akad. Nauk SSSR Ser. Fiz.* **238**, 1097 (1979).

⁸A. A. Abrikosov, L. P. Gor'kov, and I. E. Dzialoshinskii, *Methods of Quantum Field Theory in Statistical Physics* (Pergamon, New York, 1965).

⁹A. Ishimaru, *Wave Propagation and Scattering in Random Media* (Academic, New York, 1978), Vol. 1.